JCI insight

RESEARCH ARTICLE

Cytometry TOF identifies alveolar macrophage subtypes in acute respiratory distress syndrome

Eric D. Morrell,[1] Alice Wiedeman,[2] S. Alice Long,[2] Sina A. Gharib,[1] T. Eoin West,[1] Shawn J. Skerrett,[1] Mark M. Wurfel,[1] and Carmen Mikacenic[1]

[1]Division of Pulmonary, Critical Care, and Sleep Medicine, Department of Medicine, University of Washington, Seattle, Washington, USA. [2]Translational Research Program, Benaroya Research Institute at Virginia Mason, Seattle, Washington, United States of America.

Studies in human peripheral blood monocyte–derived macrophages in vitro have shown clear evidence that multiple macrophage polarization states exist. The extent to which different alveolar macrophage (AM) polarization states exist in homeostasis or in the setting of severe injury such as acute respiratory distress syndrome (ARDS) is largely unknown. We applied single-cell cytometry TOF (CyTOF) to simultaneously measure 36 cell-surface markers on CD45$^+$ cells present in bronchoalveolar lavage from healthy volunteers, as well as mechanically ventilated subjects with and without ARDS. Visualization of the high-dimensional data with the t-distributed stochastic neighbor embedding algorithm demonstrated wide diversity of cell-surface marker profiles among CD33$^+$CD71$^+$CD163$^+$ AMs. We then used a κ-nearest neighbor density estimation algorithm to statistically identify distinct alveolar myeloid subtypes, and we discerned 3 AM subtypes defined by CD169 and PD-L1 surface expression. The percentage of AMs that were classified into one of the 3 AM subtypes was significantly different between healthy and mechanically ventilated subjects. In an independent cohort of subjects with ARDS, *PD-L1* gene expression and *PD-L1/PD-1* pathway–associated gene sets were significantly decreased in AMs from patients who experienced prolonged mechanical ventilation or death. Unsupervised CyTOF analysis of alveolar leukocytes from human subjects has potential to identify expected and potentially novel myeloid populations that may be linked with clinical outcomes.

Introduction

Acute respiratory distress syndrome (ARDS) is present in 10.4% of all patients admitted to an intensive care unit worldwide (1). Despite advances in supportive care that have improved 28-day mortality to 33% (2–4), the identification of effective therapies remains elusive. Alveolar macrophages (AMs) are the most abundant leukocyte in the homeostatic human lung and are thought to possess significant phenotypic plasticity and functional heterogeneity. As a result, recently proposed models of ARDS pathogenesis have described a key role for AMs in coordinating many of the inflammatory and reparative processes that occur in the alveolar space after lung injury (5, 6).

In murine models of acute lung injury, AMs exhibit a wide spectrum of phenotypes (7, 8). However, very little is currently known about human AM phenotypes in both health and ARDS. This is partly due to the limited availability of human alveolar cells, given the need for invasive bronchoscopic sampling (5). Analytic constraints have also hampered the resolution of AM subtypes. Until recently, multicolor flow cytometry has been the analytic modality of choice, but it has been limited to measuring approximately 8 parameters because of the need to account for spectral overlap (9). Furthermore, the intensity of autofluorescence in lung macrophages can interfere with spectral analysis. These inherent limitations of studying human AMs by flow cytometry have led to contradictory reports regarding the identity of AM subtypes in ARDS. For instance, Rosseau et al. used a 7-parameter flow cytometry panel to examine bronchoalveolar lavage (BAL) samples from subjects with and without ARDS (10). They found increased BAL cell counts of HLA-DR^{hi} AMs in non-ARDS subjects compared with ARDS patients, whereas ARDS subjects had increased BAL cell counts of HLA-DR^{lo} monocytes (MONOs). Alternatively, Brittan et al. used an 8-parameter flow cytometry

Authorship note: MMW and CM contributed equally to this work.

Conflict of interest: The authors have declared that no conflict of interest exists.

Submitted: December 15, 2017
Accepted: April 13, 2018
Published: May 17, 2018

Reference information:
JCI Insight. 2018;3(10):e99281.
https://doi.org/10.1172/jci.insight.99281.

panel on human BAL samples collected from healthy volunteers and reported that inhaled LPS promoted an increase in HLR-DR^{hi} MONOs in exposed subjects compared with subjects exposed to inhaled saline (11). The use of a broader array of AM markers might resolve conflicting reports such as these that arise due to the merging of distinct cell types into single populations when insufficient phenotyping parameters are available.

Cytometry TOF (CyTOF) is an emerging technology that combines elements of flow cytometry with elemental mass spectrometry (12). Cellular proteins are first labeled with antibodies that are conjugated with heavy metals, and the identity of each labeled protein is then resolved through TOF mass spectrometry on each individual cell. CyTOF provides a highly parameterized single-cell immunophenotyping platform that circumvents some of the inherent limitations of multicolor flow cytometry of AMs, including spectral overlap and autofluorescence. The identification of granular AM subtypes could clarify our understanding of ARDS pathogenesis and may ultimately lead to the identification of novel AM molecular targets that might be used to improve ARDS outcomes. Here, we report the first application of CyTOF to our knowledge to identify extensive immunophenotypic profiles of human alveolar myeloid cells in critical illness. We hypothesized that multiple and distinct human AM subtypes exist and that these subtypes would be associated with the clinical condition of the subject from which they were obtained.

Results

Subject characteristics. Characteristics of subjects from our Harborview Medical Center BAL (HMC-BAL) and ARDS AM Gene Expression (ARDS-AMGE) study cohorts are shown in Table 1. Non-ARDS subjects in HMC-BAL were intubated and supported with mechanical ventilation due to respiratory failure from congestive heart failure or an inability to protect their airway. Samples in HMC-BAL were excluded if there was microbiologic evidence of pulmonary infection. One ARDS subject in HMC-BAL had a clinical diagnosis of pneumonia and was actively receiving antibiotics; however, collected BAL fluid did not meet microbiologic criteria for infection (less than 1×10^4 CFUs per milliliter of BAL fluid of a known pathogen) (13). ARDS-AMGE included any subject with ARDS, irrespective of infection status, and pneumonia was an ARDS risk factor in 30% of subjects.

Conventional gating of CyTOF data can resolve alveolar leukocyte populations. To identify subtypes of alveolar leukocytes in health and critical illness, we developed a CyTOF antibody panel containing 36 cell-surface markers (Supplemental Table 1; supplemental material available online with this article; https://doi.org/10.1172/jci.insight.99281DS1), stained human alveolar samples with this panel, and analyzed the samples with CyTOF. We first distinguished common alveolar leukocyte populations within intact, singlet, live, and CD45$^+$ cells (Supplemental Figure 1) using a conventional biaxial gating strategy proposed for flow cytometry–based identification of alveolar cells (9, 10). By applying this gating strategy to our CyTOF data, we categorized multiple alveolar leukocyte populations, including CD3$^+$ T cells, CD206^{lo}CD14$^+$ MONOs, CD33$^+$FceR1a^{hi} IgE–receptor positive myeloid cells, and CD33$^+$CD71$^+$CD163$^+$ AMs (Figure 1A). We removed neutrophils (PMNs) from each lavage sample as part of our cryopreservation protocol, which explains the low frequency of CD15$^+$ alveolar PMNs in our CyTOF analyses compared with percent PMN counts identified at the time of sample acquisition by cytospin examination (Table 1). These findings demonstrated that our supervised low-parameter approach was sufficient to identify common, well-described alveolar cell populations.

viSNE identifies phenotypic diversity among CD33$^+$CD71$^+$CD163$^+$ AMs. We next wanted to determine whether the use of all the markers in our panel could elucidate phenotypic heterogeneity within the conventionally defined populations outlined in Figure 1A. It is challenging to meaningfully interpret 36 simultaneously measured parameters on individual cells by using conventional biaxial gating. Therefore, we performed complexity reduction and visualization of our CyTOF data using viSNE (14). viSNE uses a computational algorithm based on the Barnes-Hut implementation of the t-distributed stochastic neighbor embedding (t-SNE) technique, reducing high-dimensional data into a single 2-dimensional biaxial plot for visualization. Each dot in the viSNE plot represents an individual cell, and the position of each dot is determined by the expression of all markers measured on that cell.

Unsupervised clustering of our CyTOF data with viSNE identified cell populations that were consistent with the conventionally gated populations shown in Figure 1A, such as T cell subsets, CD206^{lo}CD14$^+$ MONOs, and CD33$^+$CD71$^+$CD163$^+$ AMs (Figure 1B). We then created sample overlays of our viSNE plots to determine whether CD33$^+$CD71$^+$CD163$^+$ AMs from each of the 3 clinical

Table 1. Subject characteristics

		HMC-BAL		ARDS-AMGE
	Healthy (n = 4)	Non-ARDS (n = 6)	ARDS (n = 6)	ARDS (n = 30)
Demographic				
Age	22 ± 3	46 ± 11	50 ± 17	44 ± 6
Sex (M/F)	1/3	5/1	3/3	18/12
Mechanically ventilated	No	Yes	Yes	Yes
Days of mechanical ventilation prior to BAL	N/A	6.2 ± 2.4	3.5 ± 1.7	<2.0
Clinical diagnosis, *n* (%)				
ARDS	N/A	–	6 (100%)	30 (100%)
Heart failure	N/A	2 (33%)	–	–
Airway protection	N/A	4 (66%)	–	–
ARDS risk, *n* (%)[A]				
Trauma	N/A	1	3 (50%)	14 (47%)
Sepsis	N/A	–	–	17 (57%)
Pneumonia	N/A	–	1 (17%)	9 (30%)
Aspiration	N/A	–	2 (33%)	4 (13%)
Physiologic				
P/F ratio	N/A	256 ± 139	107 ± 23	198 ± 61
APACHE II	N/A	–	–	21 ± 6
APACHE III	N/A	75 ± 17	91 ± 40	–
Cellular (cytospin)				
% AM	90% ± 4%	94% ± 5%	43% ± 26%	54% ± 31%
% Neutrophil	1% ± 0%	2% ± 4%	54% ± 27%	41% ± 33%

All values are expressed as mean ± SD. Days of mechanical ventilation: number of days elapsed from initiation of mechanical ventilation to sample acquisition by bronchoalveolar lavage (BAL). AM, alveolar macrophage; APACHE, acute physiologic and chronic health evaluation; ARDS, acute respiratory distress syndrome; ARDS-AMGE, ARDS AM Gene Expression Cohort; HMC-BAL, Harborview Medical Center BAL Cohort; P/F ratio, PaO_2/FiO_2 ratio. [A]Risk factors for ARDS are not mutually exclusive.

populations (heathy, non-ARDS, and ARDS) were phenotypically distinct. We found that the $CD33^+CD71^+CD163^+$ AMs from each of the 3 clinical populations formed distinct clusters (Figure 1C), suggesting that AM subtypes might be influenced by the environment (clinical condition) to which the cells were exposed.

The addition of CyTOF data from 2 peripheral blood mononuclear cell (PBMC) samples from healthy volunteers to our 16 alveolar samples did not modify the number of clusters identified by viSNE, implying that the major leukocyte populations present in the peripheral circulation were represented in the alveolar space (Supplemental Figure 2, A and B). T cells identified from the alveolar space and peripheral blood phenotypically overlapped (Supplemental Figure 2, C and D). We also found that alveolar MONO populations were phenotypically similar to MONOs isolated from the peripheral blood based on their cluster designation within the overall viSNE plot and were only present in the BAL fluid from subjects with ARDS. There were no $CD33^+CD71^+CD163^+$ AM-like cells present in the peripheral blood.

X-Shift defines expected and potentially novel alveolar myeloid cell populations. The application of viSNE to our HMC CyTOF dataset identified extensive phenotypic heterogeneity within the $CD33^+CD71^+CD163^+$ AM population (Figure 1C). Next, we sought to more rigorously discern AM subtypes using X-Shift (15). X-Shift is a clustering algorithm that employs a computationally robust approach to cluster assignment that is based on a modified weighted κ-nearest neighbor density estimation (κNN-DE). We first removed $CD3^+$ T cells and MONOs ($CD206^{lo}CD14^+$) from our HMC-BAL dataset by manual gating (Figure 1A) and then applied X-Shift to all remaining alveolar leukocytes. κNN-DE cluster analysis of the remaining alveolar leukocytes identified 8 distinct myeloid clusters that are displayed in the Divisive Marker Tree (DMT) (Figure 2). The DMT starts with a Root node encompassing all clusters and then progresses through successive binary divisions that resemble manual gating hierarchies. For each division, the marker that has the largest variance-normalized difference between the 2 sister clusters is identified.

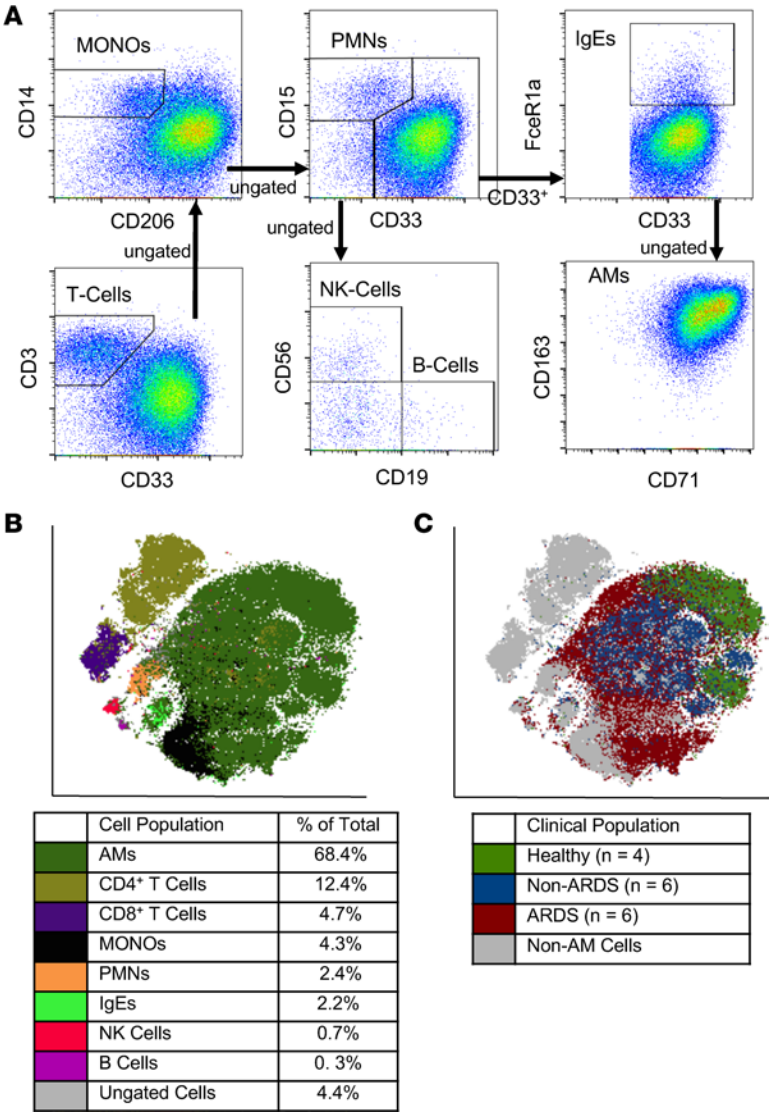

Figure 1. CyTOF analysis of leukocytes from bronchoalveolar lavage (BAL) fluid identifies common populations in an unsupervised fashion. (**A**) Biaxial gating of intact, singlet, live, and CD45$^+$ cells from 16 alveolar samples analyzed by CyTOF identifies common alveolar leukocyte populations. (**B**) Concatenated viSNE plot generated from the same data represented in **A**. The color of each dot represents its immune cell subset, as designated by manual gating shown in **A**. (**C**) Concatenated viSNE plot of all CD33$^+$CD71$^+$CD163$^+$ AMs colored per the clinical population from which each sample was procured. AM, alveolar macrophage; IgE, IgE-expressing cells (eosinophil, basophil, and mast cells); MONO, monocyte; PMN, neutrophil.

We identified 8 clusters (e.g., AM-1) based on the marker intensity distribution of each cluster interpreted within the context of prior literature (5). For example, we labeled the PMN cluster given its high expression of CD15 and low expression of CD206 (Figure 3). Supplemental Table 2 shows the marker intensities for all 36 markers. The UNK subtype represented a cluster that did not have high expression of any of the myeloid markers except CD45, suggesting that it is a population defined by markers that were not included in our panel.

DMT identified 3 distinct clusters that contained CD45RA^{lo}CD15^{lo}CD33^{hi} alveolar myeloid cells (after excluding CD3$^+$ T cells and CD206^{lo}CD14$^+$ MONOs), which we classified as AMs based on our interpretation of the cluster marker intensities (Figure 3). The markers that had the largest variance-normalized difference among these 3 AM subtypes were CD169 and PD-L1 (Figures 2 and 3, Supplemental Figure 3). To confirm that CD169 and PD-L1 are discriminating AM subtype markers that are robust to small variations in how AMs are defined, we applied X-Shift to manually gated CD33$^+$CD71$^+$CD163$^+$ AMs from our HMC-BAL data. X-Shift again identified 3 AM subtypes that were best distinguished from each other by CD169 and PD-L1 expression (Supplemental Figure 4).

CD169 and PD-L1 distinguish AM subtypes. To facilitate the translation of our high-parameter CyTOF findings into low-parameter flow cytometry workflows, we applied the DMT-derived gating hierarchy in Figure 2 to conventional biaxial plots of our HMC-BAL data (Figure 4A). We then manually divided the CD45RA^{lo}CD15^{lo}CD33^{hi} AM population based on CD169 and PD-L1 expression (Figure 4B). The percentage of AMs that were classified into one of the 3 AM subtypes was significantly different between nonmechanically ventilated and mechanically ventilated critically ill subjects (Figure 4C). Differences in these subtypes among the mechanically ventilated patients suggested a difference between those with and without ARDS; however, this difference did not meet our predetermined threshold for statistical significance (Figure 4D).

AM PD-L1 gene expression and PD-L1/PD-1 pathway–associated gene sets are associated with ventilator-free days in ARDS. Our CyTOF analyses demonstrated a clear difference in the prevalence of AM subtypes defined by CD169 and PD-L1 in healthy controls as opposed to critically ill patients with respiratory failure on mechanical ventilation. There was a numerical trend suggesting a difference between these AM subtypes among patients with and without ARDS. Next, we sought evidence of links between AM expression of markers defining these AM subtypes (CD169, PD-L1, CD71, CD86, and CD14) and severity of ARDS using previously obtained genome-wide expression measurements from AMs purified from the BAL fluid of patients (n = 30) with early ARDS (<48 hours after mechanical ventilation was initiated). These patients had been enrolled in a randomized clinical trial of fish oil for treatment of ARDS (16). These 5 genes were selected based on our CyTOF analyses

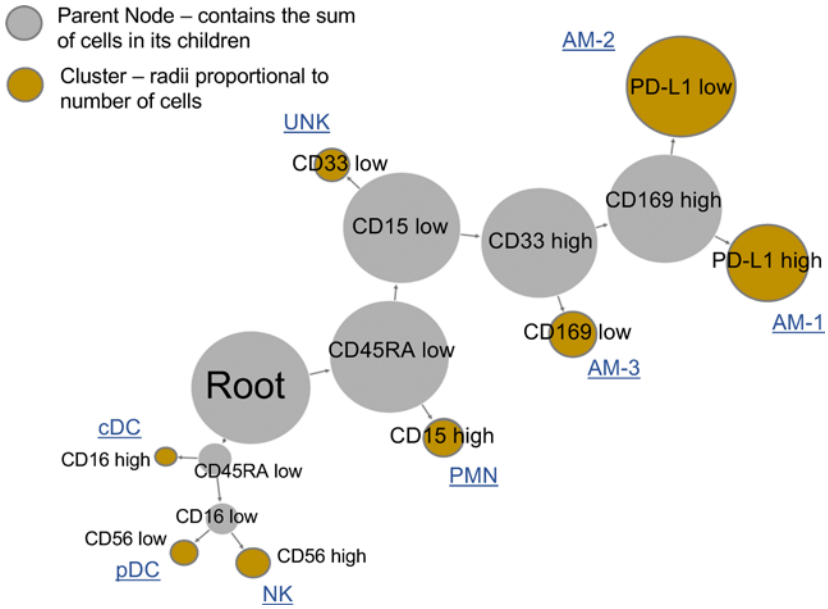

Figure 2. Unsupervised clustering by X-Shift identifies alveolar macrophage (AM) subtypes. The Divisive Marker Tree (DMT) dendrogram displays the 8 myeloid clusters derived by κNN-DE clustering (κ-nearest neighbors = 30) of alveolar myeloid cells after exclusion of $CD3^+$ T cells and $CD206^{lo}CD14^+$ MONOs. The DMT starts with the Root node encompassing all clusters and then progresses through successive binary divisions that are chosen to maximize the average uncentered Pearson correlation of each of the cluster expression profiles. For each division, the marker that has the largest variance-normalized difference between the 2 sister clusters is labeled (Supplemental Figure 3 displays the cut-off values). X-Shift performed the κNN-DE clustering and DMT tree derivation (15). cDC, conventional dendritic cell; pDC, plasmacytoid DC; PMN, neutrophil; UNK, unclassified.

showing a wide variance in median intensity between each of the 3 AM subtypes (Figure 3, red). We tested for associations between the expression level of each gene and the ARDS-related outcome, ventilator-free days (VFDs). VFDs is a composite endpoint used in ARDS clinical trials that measures the duration of need for mechanical ventilation while accounting for patient survival (17). VFDs were dichotomized about the median and classified as high VFDs (VFD ≥ 18, $n = 15$) versus low VFDs (VFD < 18, $n = 15$).

We found that AMs from individuals who experienced high VFDs had significantly higher *PD-L1* gene expression than subjects who experienced low VFDs ($P = 0.0005$) (Figure 5). The difference between the 2 groups persisted when we analyzed subjects in the active drug (fish oil) and placebo groups separately (Supplemental Figure 5, A and B). We also had gene expression measurements for a subset of patients at day 4 after enrollment, and we found no significant difference in AM *PD-L1* gene expression between the high and low VFD groups at this time point (Supplemental Figure 6). None of the transcripts for the 4 other AM-subtype markers differed between the high and low VFD groups (Figure 5).

We then expanded our analysis to genome-wide AM expression measurements. We tested whether AM *PD-L1/PD-1* or *CD86/CTLA-4* transcriptional pathways were associated with VFDs in ARDS-AMGE in samples obtained <48 hours after ARDS onset. We compiled PD-1 and CTLA-4 pathway signaling gene sets from the Molecular Signatures Database (MSigDB; http://software.broadinstitute.org/gsea/msigdb/genesets.jsp), and applied Gene Set Enrichment Analysis (GSEA; http://software.broadinstitute.org/gsea/index.jsp) to our ARDS-AMGE cohort to determine whether there was significant enrichment of these gene sets in our high versus low VFD groups (18). We found significant enrichment of the *PD-L1/PD-1* pathway gene set in high VFD versus low VFD subjects in ARDS-AMGE ($P < 0.001$) (Table 2 and Supplemental Figure 7).

Discussion

A more precise assessment of alveolar cell subtypes in human health and disease is needed to more completely understand pathophysiology and develop better therapeutics. To this end, we report the first study to our knowledge to employ CyTOF to phenotype human alveolar myeloid cells. Using clinical samples obtained by bronchoscopic sampling of healthy volunteers breathing spontaneously and critically ill mechanically ventilated subjects with and without ARDS, we have shown that human AMs possess considerable phenotypic diversity, as measured by a broad panel of cell-surface markers (Figure 1). Furthermore, we have shown that the prevalence of certain AM subtypes differs according to whether a subject is spontaneously breathing or is critically ill and supported on mechanical ventilation (Figure 4). Specifically, we identified expected ($CD33^+CD71^+CD163^+$) and potentially novel AM populations ($CD169^{hi}PD\text{-}L1^{hi}$) in an unsupervised fashion using high-parameter analysis of CyTOF data derived from alveolar leukocytes (Figure 2). In an independent cohort of subjects with ARDS, we showed that *PD-L1* gene expression and *PD-L1/PD-1* pathway–associated gene sets were significantly decreased in AMs from patients who experienced

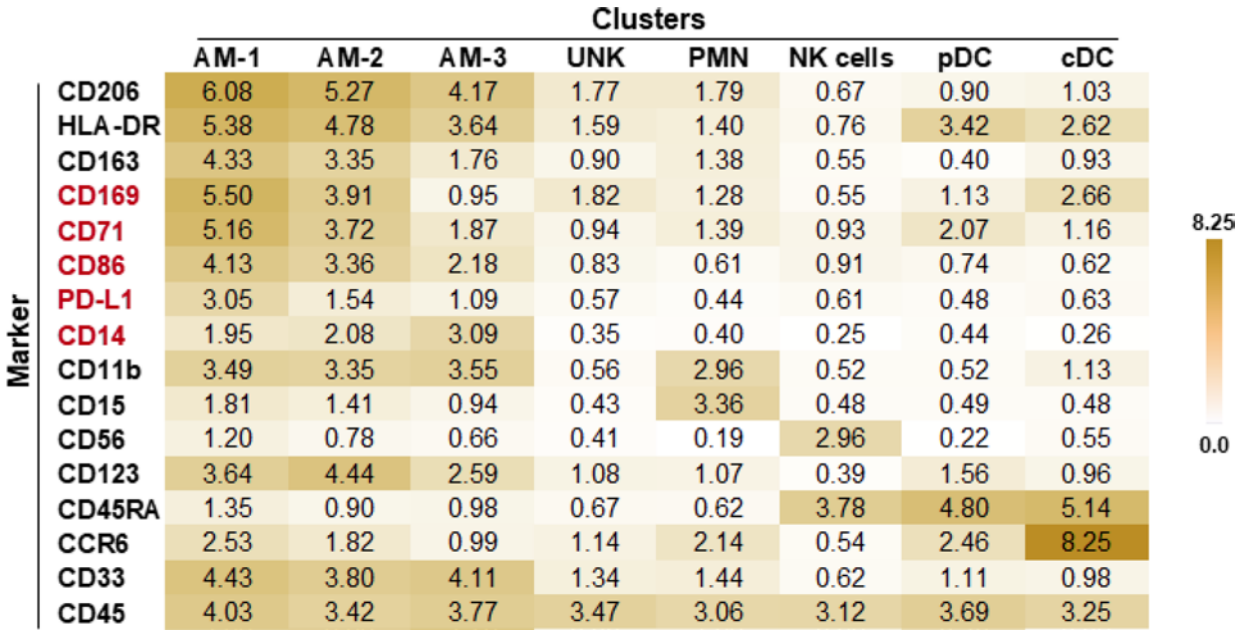

Figure 3. Most informative median myeloid marker intensities for each subtype identified by κNN-DE in HMC-BAL. All values are expressed on the arcsinh (raw intensity/5) scale. Alveolar macrophage (AM) markers colored in red were carried forward for further analysis. Figure expresses data derived from *n* = 16 total alvoelar samples (HMC-BAL). κNN-DE, κ-nearest neighbor density estimation; cDC, conventional DC; pDC, plasmacytoid DC; PMN, neutrophil; UNK, unclassified.

prolonged mechanical ventilation or death, suggesting that AM expression of this protein might be linked with clinical outcomes (Figure 5 and Table 2). Taken together, our findings are consistent with a model in which critical illness and ARDS lead to development of specific AM subtypes (5, 6). We hypothesize that these AM subtypes may help to regulate injury and repair pathways in the lungs of these patients. This model is supported by findings in murine models of acute lung injury and infection (7, 8) and suggests that distinct AM subtypes might be differentially targeted in critical illness and ARDS as a novel therapeutic approach.

Our findings add significant clarity to a prior AM phenotyping study in ARDS performed using flow cytometry that classified nonlymphocytic alveolar mononuclear cells as being either AMs or MONOs, respectively (10). Rosseau et al. compared cells obtained from serial BALs from patients with and without ARDS controls (10). They showed that persistence of MONOs in the alveolar space was associated with worse clinical outcomes compared with subjects whose BAL showed higher numbers of $CD71^{+}CD163^{+}$ AMs over the course of ARDS (10). We likewise found increased percentages of pure MONOs in our ARDS (11.5% of non-$CD3^{+}$ cells) versus healthy and non-ARDS subjects (0.41% of non-$CD3^{+}$ cells). However, even after gating out pure MONOs from our samples based upon a recently validated flow cytometry gating strategy (Figure 4A) (9), we still identified 3 distinct AM subtypes among either $CD45RA^{lo}CD15^{lo}CD33^{hi}$ (Figure 2) or $CD33^{+}CD71^{+}CD163^{+}$ cells (Supplemental Figure 4). Our findings suggest that Rosseau's flow cytometry study (10) may have consolidated distinct AM subtypes into either mature $CD33^{+}CD71^{+}CD163^{+}$ AM or MONO populations. Moreover, our identification of CD169 and PD-L1 as discriminating AM subtype markers (Figure 2) provides a basis for larger studies in humans testing whether nonmonocytic AM subtypes are associated with clinical outcomes in ARDS.

Limited data exists regarding cell-surface expression of PD-L1 or CD169 on human AMs in ARDS; however, studies have characterized an important role for these molecules in other pulmonary disease states and cell types. PD-L1 is present on most antigen presenting cells and associates with PD-1 on lymphocytes (19). PD-L1 inhibits the pro-inflammatory activity of $CD4^{+}$ and $CD8^{+}$ T cells, and lung tissue macrophage PD-L1 cell surface expression is decreased in inflammatory conditions, such as chronic obstructive pulmonary disease (20). The strong constitutive expression of PD-L1 is consistent with the role that quiescent AMs may play in suppressing inappropriate inflammation in the homeostatic human lung. Notably, PD-L1 blockade is associated with the development of an ARDS-like pneumonitis in cancer patients who are

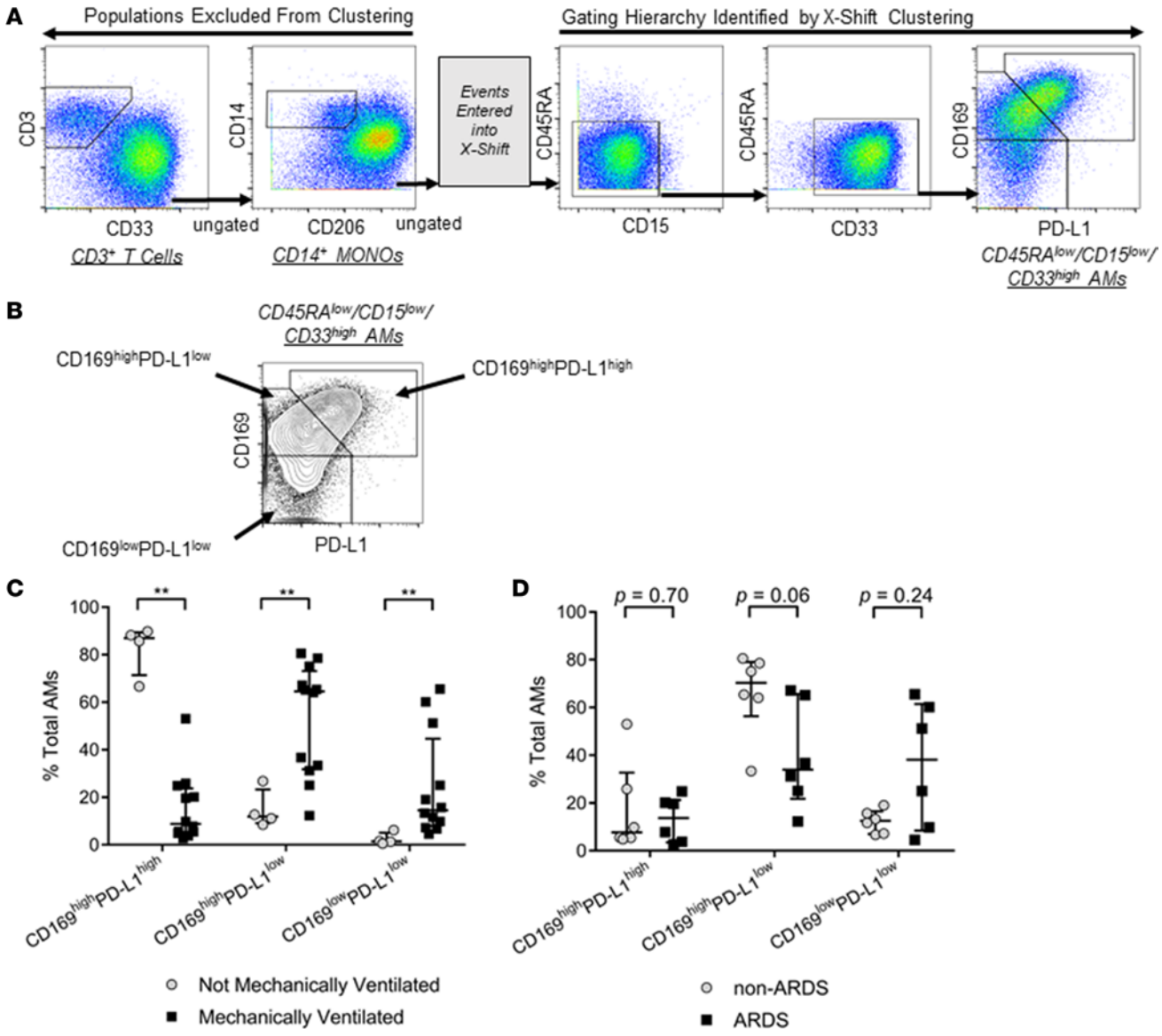

Figure 4. CD169 and PD-L1 distinguish alveolar macrophages (AMs) procured from different clinical populations. (**A**) The hierarchical gating strategy used to identify AMs is based on the Divisive Marker Tree (DMT) shown in Figure 2. (**B**) Contour plot demonstrating the manually drawn gates for CD169 and PD-L1 AM subtypes within all CD45RA^{lo}CD15^{lo}CD33^{hi} events from all 16 alveolar samples in the HMC-BAL cohort. (**C**) The population frequency of each CD169/PD-L1 AM subtype was different between nonmechanically ventilated healthy subjects and mechanically ventilated critically ill subjects (n = 4 not mechanically ventilated, n = 12 mechanically ventilated). (**D**) The population frequency of each CD169/PD-L1 AM subtype suggested a difference between non-ARDS and ARDS subjects (n = 6 non-ARDS, n = 6 ARDS). Shown are the individual values and median ± interquartile range (IQR) population frequencies of each AM subtype among total CD45RA^{lo}CD15^{lo}CD33^{hi} AMs. Each comparison was made with a Mann-Whitney U test. $^{**}P \leq 0.01$.

treated with PD-L1 checkpoint inhibitors (21, 22), suggesting that this pathway may be important to ARDS pathogenesis. Our findings in an independent cohort of patients with ARDS demonstrating decreased AM *PD-L1* gene expression and *PD-L1/PD-1* AM gene set enrichment in subjects with more severe forms of ARDS extends our CyTOF findings (Figure 5 and Table 2). Taken together, these findings suggest that AM subtypes defined by PD-L1 may be involved in the development and severity of ARDS.

Our identification of a CD169^{lo}PD-L1^{lo} AM subtype that is markedly enriched among patients with acute respiratory failure being supported by mechanical ventilation is potentially novel. However, based on prior studies, we hypothesize that the CD169^{lo}PD-L1^{lo} AM subtype is similar to a recently described pulmonary macrophage subtype. Yu et al. identified the macrophage subtype in the interstitial space of healthy human lungs (9). This CD169^{lo} interstitial-associated macrophage was strongly CD206^{+} and CD14^{+}, and it interdigitated with alveolar epithelial cells. Our CD169^{lo}PD-L1^{lo} AM-3 subtype is likewise strongly CD206^{+}

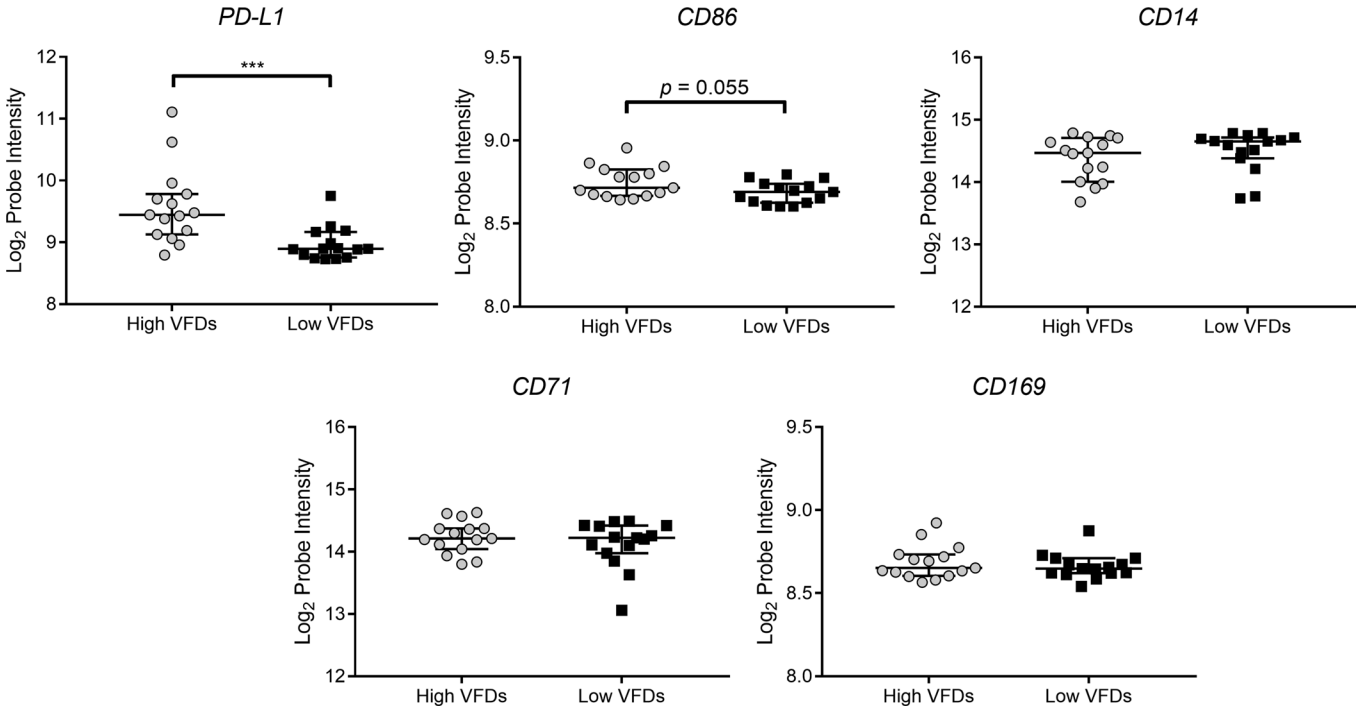

Figure 5. *PD-L1* gene expression is associated with ventilator-free days (VFDs) in subjects with acute respiratory distress syndrome (ARDS). Alveolar macrophages (AMs) were isolated <48 hours after the development of ARDS by negative selection in the ARDS-AMGE sample set. High VFDs indicate VFD ≥ 18 (n = 15) and Low VFDs indicate VFD < 18 (n = 15). mRNA normalized $\log_2$ probe intensity for each transcript is expressed as individual values and median ± interquartile range (IQR) for each group. For each gene, comparisons were made with a Mann-Whitney U test. ***P < 0.001.

and CD14$^+$ (Figure 3), was not present in the BAL fluid from healthy subjects, and was increasingly found in ARDS versus non-ARDS BAL fluid (Figure 4D). It is possible that this macrophage subtype is present exclusively in the subepithelial compartment during homeostasis but then leaks into the alveolar space after epithelial damage that might occur with ventilator-induced lung injury or in ARDS. Alternatively, this macrophage subtype may play a specific role in acute lung immunity and inflammation, as suggested in studies performed in macaques (23).

This study has several limitations. First, our sample size for the CyTOF studies is relatively small and will need to be verified. However, our findings using gene expression in the larger ARDS-AMGE cohort support the importance of our CyTOF results. Second, our CyTOF analyses were limited to a single time point that varied in its relation to the initiation of mechanical ventilation and the onset of ARDS. AM phenotype and function can change over time on mechanical ventilation and over the course of ARDS (10, 24). Indeed, the lack of a statistically robust difference in the AM subtype prevalence between ARDS and non-ARDS patients was likely influenced by the experimental noise introduced by the sampling time differences. Further evidence for the time-dependent changes were seen in the differences in AM *PD-L1* gene expression between ARDS subjects with high versus low VFDs at ARDS onset but lost by day 4 after

Table 2. Alveolar Macrophage (AM) *PD-1* pathway associated gene sets are enriched in high ventilator-free day (VFD) versus low VFD subjects with ARDS

Gene Set	NES	*P* value
REACTOME_PD1_SIGNALING	1.80	<0.001
BIOCARTA_CTLA4_PATHWAY	1.33	0.13

NES, normalized enrichment score. The NES is expressed in High VFD subjects (High VFDs = VFD ≥ 18, n = 15) versus Low VFD subjects (Low VFDs = VFD < 18, n = 15). The gene sets tested were obtained from the Broad Molecular Signatures Database (http://software.broadinstitute.org/gsea/msigdb/genesets.jsp).

mechanical ventilation (Supplemental Figure 6). Longitudinal studies will be required to further delineate the relationships between AM subtypes and ARDS onset and progression. Third, our findings linking differences in *PD-L1* gene expression and VFDs was only performed in patients with ARDS; thus, we cannot say to what extent this relationship is exclusive to patients with ARDS as opposed to patients with acute respiratory failure in general. Fourth, the cells obtained by BAL are not necessarily fully representative of all cells in the alveolar or interstitial space. Finally, we used cryopreserved samples to allow for batched processing of our samples to limit experimental noise from day-to-day technical variation. Our protocol was standardized across all samples collected, but it remains possible that cryopreservation may have altered measurements relative to freshly processed cells.

In summary, we have identified expected and potentially novel human AM subtypes present in ARDS that may be related to salient clinical outcomes. We suggest that there is an inflammatory AM subtype characterized by low expression of PD-L1 and CD169 in human $CD45RA^{lo}CD15^{lo}CD33^{hi}$ AMs procured from subjects with ARDS. Our study clearly demonstrates the feasibility and utility of high-dimensional single-cell analysis of alveolar samples from critically ill patients. It is likely that this approach will reveal important insights on the alveolar cells that play a key role in the development and resolution of ARDS and other forms of acute inflammatory lung disease.

Methods

Study populations. For CyTOF experiments, intubated and mechanically ventilated patients undergoing BAL for clinical suspicion of ventilator-associated pneumonia (VAP) were recruited from multiple ICUs at Harborview Medical Center in Seattle, Washington, USA. The indications and protocols for performing VAP BALs are standardized at Harborview (25). Specifically, bronchoscopy with BAL is performed to evaluate for VAP if a patient meets the following 3 criteria: (a) radiographic abnormalities; (b) 1 or more of the following clinical signs: fever, purulent endotracheal secretions, or leukocytosis; and (c) no new antimicrobial drugs for ≥72 hours. All samples from mechanically ventilated patients in HMC-BAL were obtained by bronchoscopies that were performed by a member of the clinical team caring for the patient. Our research samples were obtained from the excess total BAL fluid not needed for clinical care and processed within 1 hour of the procedure. ARDS was defined using the 2012 Berlin Definition for ARDS (26). We excluded samples if: (a) there was any microbiologic evidence of pulmonary infection (defined as $\geq 1 \times 10^4$ CFUs of a respiratory pathogen), (b) the sample did not contain >1 million alveolar cells, (c) the sample was collected >10 days after the initiation of mechanical ventilation, or (d) the sample was procured from a subject with burns, prior solid organ/stem cell transplant, active malignancy, or human immunodeficiency virus.

Healthy subjects were recruited from the Seattle metropolitan area with the following exclusion criteria: (a) age <18 or >50, (b) active tobacco use, (c) prescription medication use, or (d) any history of pulmonary, immune, or chronic illness. All healthy subjects were spontaneously breathing, BAL was performed with local anesthesia, and no sedation was administered. Frozen PBMCs were obtained from the Benaroya Research Institute Immune Mediated Disease Registry and Repository.

For gene expression experiments, data was derived from subjects with ARDS enrolled in the Fish Oil Phase-II Randomized Placebo-Controlled Trial (16). Full inclusion and exclusion criteria are described in the original manuscript. Patients randomized to both the fish oil treatment (n = 10) and placebo (n = 20) were included in our analysis. There were no differences in any of the plasma biomarker levels, BAL fluid biomarker levels, or clinical outcomes between the placebo and treatment groups in this trial (16). VFDs were defined as the number of days a subject was alive and free from mechanical ventilation between day 1 and day 28 after enrollment (17). If a subject died before day 28, he or she was considered to have VFDs of 0.

CyTOF sample processing. Alveolar samples were filtered through a 70-μm cell strainer and then centrifuged at 400 *g* for 5 minutes. The supernatant was removed and stored, and red blood cells were eliminated using a lysis buffer (BioLegend). Alveolar leukocytes were washed and resuspended in 2% FBS, and an aliquot was processed for a cytospin. The cells were washed again and then cryopreserved in 7% DMSO (Thermo Fisher Scientific).

All samples were thawed on the day of processing, incubated in 50 units/ml DNase (Benzonase Nuclease, MilliporeSigma) for 5 minutes, washed ×2 in PBS, and then stained with cisplatin (viability stain; Enzo Life Sciences) for 1 minute at room temperature. The cells were then washed and resuspended with human Fc blocker for 5 minutes (TruStain FcX, BioLegend). Samples were stained with the 36-antibody cocktai

(Supplemental Table 1) in cell staining buffer (Fluidigm) for 30 minutes at room temperature. Following incubation, cells were washed ×2 and then resuspended with MaxPar Intercalator-Ir (intact stain) in Fix and Perm Buffer (Fluidigm). Cells were washed, and then resuspended in ultrapure water to be run on the CyTOF. Stained cells were analyzed on a CyTOF (Fluidigm) at an event rate of 300–400 cells per second. We processed the samples in 2 separate batches.

Gene expression sample processing. Negative selection for AMs was achieved by incubating cells collected from BAL fluid of subjects with ARDS with antibody-labeled microbeads as previously described (27). RNA was purified using ABI Isolation of Total RNA from Cells protocol (Applied Biosciences Inc.) using the ABI Prism 6100 Nucleic Acid PrepStation. RNA purity was qualitatively assessed by an automated RNA electrophoresis chip (Bio-Rad). After RNA isolation, total RNA from each sample was amplified by performing a 2-cycle amplification process (Applied Biosciences Inc.). After amplification, biotin-labeled anti-sense complementary DNA (cDNA) was synthesized, fragmented, and hybridized to an Illumina HumanRef-8 BeadChip (Illumina Inc.) containing 24,526 unique probes (inclusive of 18,415 unique genes).

CyTOF data analysis. Prior to data analysis, all events were preprocessed in FlowJo v10 by manually gating on intact, singlet, live, and $CD45^+$ cells. All analyses after preprocessing were performed on inverse hyperbolic sine transformed data. All viSNE plots (14) were generated on equally downsampled events in Cytobank Premium (Cytobank Inc.) with the following parameters: perplexity = 30; $\theta = 0.5$; iterations = 1,000. The viSNE plots shown in Figure 1 and Supplemental Figure 2 were edited in FlowJo, and all manual gating was performed in FlowJo.

Automated clustering was performed in X-Shift (http://web.stanford.edu/~samusik/vortex) (15) on all cells remaining after $CD3^+$ T cells and $CD206^{lo}CD14^+$ MONOs were removed (Figure 2) or on all $CD33^+CD71^+CD163^+$ cells (Supplemental Figure 4) with the following parameters: minimal euclidean length of the profile = 1.0; distance measure = euclidean distance; clustering algorithm = X-Shift; density estimate = *n* nearest neighbors, κ (nearest neighbors) = 30.

Microarray data analysis. We performed variance stabilization and quantile normalization of the Illumina HumanRef-8 microarray data using the Bioconductor package *lumi* (28). Individual probe intensities were $\log_2$ transformed. We complied the REACTOME_PD1_SIGNALING and BIOCARTA_CTLA4_PATHWAY gene set lists from the MSigDB (http://software.broadinstitute.org/gsea/msigdb/genesets.jsp) and applied these gene sets to ARDS-AMGE using GSEA (18).

Statistics. Continuous percentages and normalized $\log_2$ probe intensities are presented as median values ± interquartile range (IQR). Comparisons between 2 groups were performed with a Mann-Whitney *U* test. A 2-tailed $P \leq 0.05$ was considered statistically significant. Statistics were performed with GraphPad Prism 7.0 (GraphPad Software Inc.).

Study approval. All studies were approved by the Human Subjects Division at the University of Washington. Samples obtained from critically ill patients on mechanical ventilation were obtained from discarded excess samples from clinically indicated bronchoscopies under a waiver of consent. Written informed consent was obtained from all subjects enrolled in ARDS-AMGE and healthy subjects undergoing research bronchoscopy or blood draw.

Author contributions

EDM, MMW, and CM contributed to the conception and design of the work. EDM, AW, SAL, SAG, TEW, SJS, MMW, and CM contributed to the acquisition, analysis, and interpretation of the data for the work. EDM, MMW, and CM drafted and revised the manuscript. EDM, AW, SAL, SAG, TEW, SJS, MMW, and CM significantly contributed to and approved the final version of the manuscript for publication.

Acknowledgments

This work was supported by NIH grants T32 HL007287, F32 HL138746, K23 HL120896, 1R01 AI093646, R01 HL113382, and P50 HL073997.

Address correspondence to: Carmen Mikacenic, Harborview Medical Center, 325 Ninth Avenue, Box 359640, Seattle, Washington 98104, USA. Phone: 206.897.5323; Email: cmikacenic@uw.edu.

1. Bellani G, et al. Epidemiology, Patterns of Care, and Mortality for Patients With Acute Respiratory Distress Syndrome in Intensive Care Units in 50 Countries. *JAMA*. 2016;315(8):788–800.
2. Papazian L, et al. Neuromuscular blockers in early acute respiratory distress syndrome. *N Engl J Med*. 2010;363(12):1107–1116.
3. Guérin C, et al. Prone positioning in severe acute respiratory distress syndrome. *N Engl J Med*. 2013;368(23):2159–2168.
4. Acute Respiratory Distress Syndrome Network, et al. Ventilation with lower tidal volumes as compared with traditional tidal volumes for acute lung injury and the acute respiratory distress syndrome. *N Engl J Med*. 2000;342(18):1301–1308.
5. Aggarwal NR, King LS, D'Alessio FR. Diverse macrophage populations mediate acute lung inflammation and resolution. *Am J Physiol Lung Cell Mol Physiol*. 2014;306(8):L709–L725.
6. Thompson BT, Chambers RC, Liu KD. Acute Respiratory Distress Syndrome. *N Engl J Med*. 2017;377(6):562–572.
7. Johnston LK, Rims CR, Gill SE, McGuire JK, Manicone AM. Pulmonary macrophage subpopulations in the induction and resolution of acute lung injury. *Am J Respir Cell Mol Biol*. 2012;47(4):417–426.
8. Mould KJ, et al. Cell Origin Dictates Programming of Resident versus Recruited Macrophages during Acute Lung Injury. *Am J Respir Cell Mol Biol*. 2017;57(3):294–306.
9. Yu YR, et al. Flow Cytometric Analysis of Myeloid Cells in Human Blood, Bronchoalveolar Lavage, and Lung Tissues. *Am J Respir Cell Mol Biol*. 2016;54(1):13–24.
10. Rosseau S, et al. Phenotypic characterization of alveolar monocyte recruitment in acute respiratory distress syndrome. *Am J Physiol Lung Cell Mol Physiol*. 2000;279(1):L25–L35.
11. Brittan M, et al. A novel subpopulation of monocyte-like cells in the human lung after lipopolysaccharide inhalation. *Eur Respir J*. 2012;40(1):206–214.
12. Spitzer MH, Nolan GP. Mass Cytometry: Single Cells, Many Features. *Cell*. 2016;165(4):780–791.
13. Fagon JY, et al. Invasive and noninvasive strategies for management of suspected ventilator-associated pneumonia. A randomized trial. *Ann Intern Med*. 2000;132(8):621–630.
14. Amir el-AD, et al. viSNE enables visualization of high dimensional single-cell data and reveals phenotypic heterogeneity of leukemia. *Nat Biotechnol*. 2013;31(6):545–552.
15. Samusik N, Good Z, Spitzer MH, Davis KL, Nolan GP. Automated mapping of phenotype space with single-cell data. *Nat Methods*. 2016;13(6):493–496.
16. Stapleton RD, et al. A phase II randomized placebo-controlled trial of omega-3 fatty acids for the treatment of acute lung injury. *Crit Care Med*. 2011;39(7):1655–1662.
17. Rubenfeld GD, Angus DC, Pinsky MR, Curtis JR, Connors AF, Bernard GR. Outcomes research in critical care: results of the American Thoracic Society Critical Care Assembly Workshop on Outcomes Research. The Members of the Outcomes Research Workshop. *Am J Respir Crit Care Med*. 1999;160(1):358–367.
18. Subramanian A, et al. Gene set enrichment analysis: a knowledge-based approach for interpreting genome-wide expression profiles. *Proc Natl Acad Sci USA*. 2005;102(43):15545–15550.
19. Freeman GJ, et al. Engagement of the PD-1 immunoinhibitory receptor by a novel B7 family member leads to negative regulation of lymphocyte activation. *J Exp Med*. 2000;192(7):1027–1034.
20. McKendry RT, et al. Dysregulation of Antiviral Function of CD8(+) T Cells in the Chronic Obstructive Pulmonary Disease Lung. Role of the PD-1-PD-L1 Axis. *Am J Respir Crit Care Med*. 2016;193(6):642–651.
21. Nishino M, Sholl LM, Hodi FS, Hatabu H, Ramaiya NH. Anti-PD-1-Related Pneumonitis during Cancer Immunotherapy. *N Engl J Med*. 2015;373(3):288–290.
22. Naidoo J, et al. Pneumonitis in Patients Treated With Anti-Programmed Death-1/Programmed Death Ligand 1 Therapy. *J Clin Oncol*. 2017;35(7):709–717.
23. Cai Y, Sugimoto C, Arainga M, Alvarez X, Didier ES, Kuroda MJ. In vivo characterization of alveolar and interstitial lung macrophages in rhesus macaques: implications for understanding lung disease in humans. *J Immunol*. 2014;192(6):2821–2829.
24. Steinberg KP, Milberg JA, Martin TR, Maunder RJ, Cockrill BA, Hudson LD. Evolution of bronchoalveolar cell populations in the adult respiratory distress syndrome. *Am J Respir Crit Care Med*. 1994;150(1):113–122.
25. Dellit TH, Chan JD, Skerrett SJ, Nathens AB. Development of a guideline for the management of ventilator-associated pneumonia based on local microbiologic findings and impact of the guideline on antimicrobial use practices. *Infect Control Hosp Epidemiol*. 2008;29(6):525–533.
26. ARDS Definition Task Force, et al. Acute respiratory distress syndrome: the Berlin Definition. *JAMA*. 2012;307(23):2526–2533.
27. Morrell ED, et al. Peripheral and Alveolar Cell Transcriptional Programs Are Distinct in Acute Respiratory Distress Syndrome. *Am J Respir Crit Care Med*. 2018;197(4):528–532.
28. Du P, Kibbe WA, Lin SM. lumi: a pipeline for processing Illumina microarray. *Bioinformatics*. 2008;24(13):1547–1548.